What User-Cell Association Algorithms will work best in mmWave Massive MIMO Ultra-Dense HetNets?

Sinasi Cetinkaya, Umair Sajid Hashmi, Ali Imran
Department of Electrical and Computer Engineering,
The University of Oklahoma, Tulsa, OK
Email: {sinasicetinkaya, umair.hashmi, ali.imran}@ou.edu

Abstract—With the abundance of sites and the heterogeneity in the network, optimal user-cell association which is a well known open problem will become a more challenging issue. Contrary to the current studies that address this problem for convectional HetNets with massive MIMO deployments in HF (high frequencies) ranges, in this paper we investigate user-cell association problem for dense two-tier networks with massive MIMO deployment both at macro and femto-tier operating in HF and mmWave spectrum respectively. The association problem modeled as a convex network utility maximization is a function of the downlink user throughput and is solvable through load aware user association schemes such as the centralized subgradient and distributed user-centric game-theoretic based algorithms. We show via extensive simulation results that both the centralized and user-centric approaches almost equally outperform the traditional association schemes, namely smallest pathloss and maximum data rate, in terms of downlink user throughput and load balancing. Our results exhibit average throughput gains between 20 and 40% for the majority of users if massive MIMO ultra-dense HetNet (UDHN) deployments are operated in the mmWave spectrum as compared to existing HF bands under the optimal user-cell association schemes. Contrary to the existing load aware association schemes that preclude the effect of bandwidth disparity in HF and mmWave bands, we show that the optimal user-cell association algorithms when employed with distinct bandwidths for each band yield higher average throughput in a two-tier HF-mmWave UDHN.

Index Terms—Massive MIMO, mmWave network, HetNet, user-association schemes, load balancing, proportional fairness

I. INTRODUCTION

Massive MIMO (multiple-input and multiple-output) and mmWave spectrum utilization have been identified as key enabling solutions to achieve orders of magnitude more data traffic as envisioned for 5G. Massive MIMO is a multi-user MIMO technology where each base station (BS) is equipped with an array of hundreds of active antenna elements to communicate with single-antenna user terminals that are far less in number as compared to the antenna elements at the BS. On the other hand, given the shortage of available spectrum at traditional cellular frequencies, mmWave spectrum (30 GHz -300 GHz) can be utilized to increase the available spectrum by 200 times as compared to presently allocated HF (sub 6 GHz spectrum) [1] [2]. Furthermore, the smaller wavelengths at mmWave frequencies enable large antenna arrays and spatial beamforming techniques [3] which provide array gains to counter the larger free space attenuation. Due to their smaller antenna form factors at mmWave frequency, massive MIMO antenna arrays are a viable deployment option in UDHN consisting of dense femto base stations (FBSs) tier underlaid over the relatively sparsely deployed macro base stations (MBSs).

User-cell association in UDHNs is a well-known problem, primarily due to the intertwined objective functions, such as coverage probability optimization [4], sum rate maximization [5], joint user association and power control [6] and energy efficiency [7]. The standard Reference Signal Received Power (RSRP) based user-cell association offers a highly imbalanced inter-tier load distribution in a massive MIMO UDHN due to the large array gain in the MBS tier [8]. This consequently demands incorporation of the load on rate characterization for both inter and intra-tier offloading problem [9]. With the advent of mmWave massive MIMO UDHNs, the user-cell association is further complexified due to: 1) high sensitivity of the mmWave to static blockages such as buildings, 2) increased pathloss following the Friss free-space propagation model [10] and 3) significant disparity in pathloss exponents for LOS and NLOS scenarios [11].

Recently several advanced user-cell association schemes have been proposed massive MIMO deployment in HF spectrum [12][13]. Given the contrasting beamforming designs and channel blockage effects, how well these association schemes work in a massive MIMO mmWave deployment at FBSs in terms of the throughput gain remains terra incognita. To the best of our knowledge, this paper is first attempt to investigate throughput performance of the optimal massive MIMO user-cell association algorithms in HF namely centralized subgradient (henceforth referred as CS) [12] and distributed user-centric [12] (henceforth referred as DUC) algorithms against the more standard smallest pathloss (henceforth referred as SPL) and max rate (henceforth referred as MR) schemes for a mmWave massive MIMO UDHN. The contributions and finding of this work are summarized below:

A. Contributions and Organization

- User-cell association in massive MIMO deployments in mmWave based HetNets requires understanding and incorporating the mmWave specific idiosyncracies of the channel characteristics as well as practical beamforming

strategies for each tier in dense urban environments. Keeping these factors in consideration, we adapt a system model [12] that enables a comparative analysis of the recently proposed CS and DUC schemes with the traditional approaches from the non-Massive MIMO era.

- Contrary to the user-cell association approach in [12] which is based on the optimization of bandwidth normalized user throughput, we incorporate the effect of increased bandwidth available at mmWave spectrum in the utility function that enables higher data rates and consequently higher probability for user off-loading from MBS to FBS tier.
- We perform a detailed comparative analysis of the four user-cell association schemes for the mmWave massive MIMO system and show that CS and DU outperform the traditional algorithms only when higher bandwidth at mmWave spectrum is taken into account.
- We also evaluate the throughput performance comparison against the existing massive MIMO HetNet model [12] to reveal that operating the FBSs at higher frequency spectrum (mmWave) enables throughput gains due to higher spectrum availability and stronger pathloss degradation of the interfering signals.

The rest of the paper organization is as follows: in Section II, we describe the radio propagation model and the user-cell association mechanism in the mmWave massive MIMO deployment. Sections III focusses on the CS and the DUC approaches for the optimization problem. In Section IV, we analyze and compare the performance of these algorithms for the massive MIMO deployment in HF and mmWave spectrum. The paper closes with conclusions and future research directions in Section V.

II. SYSTEM MODEL

A. Radio Environment and Parameters

We consider a two-tier system with MBSs and FBSs distributed across a 2-dimensional plane and operating in the HF and mmWave spectrum respectively. We use $j \in \mathbb{J} = \{MBS_1, MBS_2, .., MBS_M\} U \{FBS_1, FBS_2, .., FBS_F\}$ and $k \in \mathbb{K} = \{1, 2, .., K\}$ to index the BSs (combination of M MBSs and F FBSs) and users respectively. The users are assumed to be distributed across the MBS tier foot-prints in a non-homogenous manner with higher concentration within specified hotzones. The FBS distribution is modeled using an independent Poisson Point Process. This work assumes that all users in the network are served with proportional fairness (PF) and each user is served by only one BS at a time. The notations used in this paper are presented in Table I.

Due to sensitivity of wireless channel, particularly at mmWaves, to physical blockages, we estimate the LOS probability of an arbitrary user as a function of its distance with its associated FBS. Using the 3GPP model [14] and LOS ball model [15] for the HF and mmWave channels in an urban environment respectively, we estimate $P_{LOS}(d)$ for each user and assign pathloss exponents α_{LOS} and α_{NLOS} accordingly.

We assume massive MIMO deployment both at MBSs and FBSs with A_j as the number of antennas and S_j as the data downlink stream capacity per time slot at any MBS / FBS j. Using time division multiplexing (TDD), the BSs learn about the channel coefficients via the pilots transmitted by the associated users in the uplink. This allows each BS to serve a set of up to S_j associated UEs using linear zero-forcing beamforming (LZFBF) and analog beamforming in MBS and FBS tiers respectively. The beamforming gain is particularly important for the mmWave channel to offset the free space pathloss due to higher frequency and blockage effect.

For transmission, we consider OFDMA based scheme where each user schedules transmissions over contiguous time-frequency slots, also referred to as resource blocks (RBs) [16]. We use the block-fading channel model that captures the effect of both large-scale and small-scale fading. $g_{k,j}$ which denotes the pathloss and shadowing between an arbitrary BS j and user k is considered constant across all RBs. Because the HF and mmWave spectrum exhibit varying channel characteristics, we have distinct small-scale fading models for MBS-user and FBS-user channels. For the MBS-user link, the small-scale channel coefficients which are same within every OFDM RB, but not necessarily same across RBs, are modeled as Rayleigh fading coefficients. In the case of FBS-user association, the small-scale channel is modeled by independent Nakagami fading for each channel with different coefficients N_L and N_N for LOS and NLOS links. If $h_{k,j}$ represents the small-scale fading between a user k and a FBS j, then $|h_{k,j}|^2$ is a normalized Gamma random variable. However, due to the effect of channel hardening in massive MIMO systems [17], we ignore the effect of small scale channel coefficients in our model, i.e., we consider $|h_{k,j}| = 1, \forall k \in \mathbb{K}, j \in \mathbb{J}$.

We assume the load of an arbitrary BS j in a given time slot as the number of users associated with it which can be denoted by $|K_j|$. The instantaneous downlink rate for a user k served by BS j, using the notations in Table 1, is given by (see [18] for system details)

$$R_{k,j} = (1 - \frac{Q}{T}) \frac{T_u}{T_s} log_2(1 + \text{SINR}_{k,j}), \quad (1)$$

where the SINR with LZFBF at a user k associated with a macro BS j is adapted from [19] and given for a perfect CSI at j by

$$\text{SINR}_{k,j} = \frac{(\frac{A_j}{S_j} - 1) g_{k,j}^2 P_j}{\eta No + \sum_{l \in \mathbb{J}, l \neq j} g_{k,l} P_l + \sum_{l \in \mathbb{J}(q(k)) : l \neq j} (\frac{A_l}{S_l} - 1) g_{k,l}^2 P_l}. \quad (2)$$

As the number of antennas in mmWave massive MIMO increase, the implementation of digital beamforming techniques like LZFBF becomes infeasible because of higher power consumption and associated costs [20]. Therefore, using analog beamforming, the SINR value at a user k associated with a FBS j is given by [21][18]

$$\text{SINR}_{k,j} = \frac{(\frac{A_j}{S_j}) g_{k,j}^2 P_j}{\eta No + \sum_{l \in \mathbb{J}, l \neq j} G_l g_{k,l} P_l + \sum_{l \in \mathbb{J}(q(k)) : l \neq j} (\frac{A_l}{S_l}) g_{k,l}^2 P_l}, \quad (3)$$

TABLE I
NOTATION SUMMARY

Notation	Description
$\mathbb{J}, \mathbb{K}$	set of BSs (MBSs, FBSs) and single antenna UEs
S_j	number of data streams transmitted by BS j on a given slot
r_k	throughput of user k
$R_{k,j}$	instantaneous rate of user k serving by BS j
A_j	number of antennas at BS j
S_j/A_j	spatial load at BS j
$g_{k,j}$	pathloss and shadowing between BS j and user k
Q	number of symbols per slot for uplink pilots
T	number of downlink OFDM symbols per time slot
P_j	transmit power of BS j
d	distance between an arbitrary user its associated BS
B	total bandwidth
N_o	noise power
N_F	noise figure
k_b	Boltzmann's constant
T_K	temperature in degrees Kelvin
$|K_j|$	number of users served by BS j
m_{i_k}	number of migrations observed by user k in i-th iteration
p	switching probability

where

$$G_l = \begin{cases} \frac{A_l}{S_l}, & \text{with probability } \frac{1}{\sqrt{A_l}} \\ \frac{1}{\sin^2\left(\frac{3\pi}{2\sqrt{A_l/S_l}}\right)}, & \text{with probability } \left(1 - \frac{1}{\sqrt{A_l}}\right) \end{cases} \cdot (4)$$

In (1), Q is defined as number of symbols per slot for uplink pilots and T is the total number of OFDM symbol within each time slot. $\frac{T_u}{T_s}$ is the ratio of useful symbol duration to the total symbol duration and considered unity without any loss of generality. In (2) and (3), $\eta \geq 1$, which is the normalizing factor that guarantees that no BS infringes power constraints [18]. (4) expresses the relative power radiated by the interfering BS l in the direction of the user k served by BS j [21]. Finally, the user throughput is expressed as

$$r_k = \sum_{j \in \mathbb{J}} B_j \alpha_{k,j} R_{k,j}, \ \forall \ k \in \mathbb{K}, \tag{5}$$

where $\alpha_{k,j} = S_j/|K_j| \in [0,1]$ represents the activity fraction of RBs allocated to user k by the serving BS j. The system noise power is given by $N_0 = N_F k_b T_K B$.

B. Problem Formulation for Optimal User Cell Association

In the conventional cellular wireless networks, association decisions are performed based on RSRP (or RSRQ) levels, where each user is connected to the BS which offers best received power without considering the load of BSs. However, this approach is not optimal, particularly if we consider heterogeneity in the future wireless networks. A drawback of this scheme is that even though FBSs are usually located in areas with higher user densities (hot-zones), users tend to connect to MBSs with max RSRP association because of their higher transmit power as compared to FBSs. This calls for an offloading or load balancing mechanism which forces the users to associate with lightly loaded FBSs for efficient utilization of the available RBs.

In massive MIMO systems, the large antenna arrays significantly improve the SINR and subsequently instantaneous rates due to array gains [21]. This motivates the use of MR association scheme, in which an arbitrary user k is associated with BS j based on the achievable downlink rate given by the product of bandwidth allocated to j and the instantaneous rate given by (1), i.e $B_j * R_{k,j}$. It is further shown in [12] that CS and DUC based user-association schemes outperforms MR in terms of 5 percentile throughput while MR still achieves higher average throughput with the associated caveat of imbalanced inter-tier load distributions. Whether MR still outperform CS and DUC for mmWave UDHN remains an open question. As mmWave network exhibits noise-limited behaviour, some have proposed the SPL model (user k is associated with BS j based on smallest pathloss; expressions for each scenario are given in table II) for user-cell association [22]. For the sake of completeness, we will compare the performance of the CS (Sections II, III) and DUC (Section III) algorithms with these baseline association schemes (Section IV).

We assume PF in the problem formulation in order to allocate more RBs to users with stronger downlink channels. In this regard, we assume the utility function as $U(r) = \sum_k \log r_k$. The load aware throughput maximization problem [12] that manifests a logarithmic utility function has been adjusted to cater for inter-tier bandwidth disparity as:

$$\max_{\alpha, r} U(\mathbf{r}) \tag{6a}$$

s.t.

$$r_k \leq \sum_{j \in \mathbb{J}_k} B_j \alpha_{k,j} R_{k,j}, \quad \forall \ k \in \mathbb{K} \tag{6b}$$

$$\sum_{k \in \mathbb{K}} \alpha_{k,j} \leq S_j, \quad \forall \ j \in \mathbb{J} \tag{6c}$$

$$\sum_{j \in \mathbb{J}} \alpha_{k,j} \leq 1, \quad \forall \ k \in \mathbb{K} \tag{6d}$$

$$r_k \geq 0, \quad \alpha_{k,j} \geq 0. \quad \forall \ k \in \mathbb{K}, j \in \mathbb{J}. \tag{6e}$$

The constraint (6c) in the maximization framework limits the total activities of the users attached to BS j to be within the downlink data streams S_j. Similarly, constraint (6d) states that in case of multiple BS associations to a single user, the limit of the sum of activities of the all the BSs which serve a user k cannot exceed unity. Note that (6d) makes the problem (6) different from the classical unique association problem formulation, in which each user can only be served by one BS at max. However, the solution of (6) gives a feasible upper bound benchmark to any user-cell association which enforces unique association [12]. Finally, constraint (6e) ensures that no user is suffering from zero throughput, i.e. all admitted users have positive downlink data rates. The defined user association problem (6) is known to be convex with the solution providing an optimally feasible association configuration [12].

III. LOAD AWARE USER-CELL ASSOCIATION SCHEMES

A. Langrangian Dual analysis and Centralized Subgradient algorithm based solution

For the solution of (6), the Langrangian duality function is similar to equation 10 in [12] and can be expressed as

$$L(\boldsymbol{\alpha}, \boldsymbol{r}, \boldsymbol{\omega}, \boldsymbol{\mu}, \boldsymbol{\nu}) = U(\boldsymbol{r}) - \sum_k \omega_k (r_k - \sum_j B_j \alpha_{k,j} R_{k,j})$$
$$- \sum_j \mu_j (\sum_k \alpha_{k,j} - S_j) - \sum_k \nu_k (\sum_j \alpha_{k,j} - 1), \quad (7)$$

where $\boldsymbol{r} \geq 0$ and $\boldsymbol{\alpha} \geq 0$ are the primal variables and $\boldsymbol{\omega}, \boldsymbol{\mu}, \boldsymbol{\nu}$ are the Lagrange multipliers. The dual function $\boldsymbol{G}$ in (8) is the maximum of Lagrangian function over $\boldsymbol{\alpha}$ and $\boldsymbol{r}$ and can be minimized over the feasible set of dual variables to give the optimal global solution of the convex problem (9).

$$G(\boldsymbol{\omega}, \boldsymbol{\mu}, \boldsymbol{\nu}) = \max_{\boldsymbol{r}, \boldsymbol{\alpha}} L(\boldsymbol{\alpha}, \boldsymbol{r}, \boldsymbol{\omega}, \boldsymbol{\mu}, \boldsymbol{\nu}). \quad (8)$$

$$\min G(\boldsymbol{\omega}, \boldsymbol{\mu}, \boldsymbol{\nu}), \quad s.t. \ \boldsymbol{\omega}, \boldsymbol{\mu}, \boldsymbol{\nu} \geq 0. \quad (9)$$

The optimal solution of the convex problem in (9) that maximizes the throughput r_k is given by [1]

$$\min \sum_j S_j \mu_j + \sum_k \nu_k - \sum_k log(\min_j \{\frac{\mu_j + \nu_k}{B_j R_{k,j}}\}), \quad (10)$$

where $\boldsymbol{\mu}, \boldsymbol{\nu} \geq 0$. The modified dual problem in (10) is a convex function of dual variables $(\boldsymbol{\mu}, \boldsymbol{\nu})$ since the second partial derivatives with dual variable $\boldsymbol{\mu}$ and $\boldsymbol{\nu}$ exists with a non-negative value [21]. Based on above analysis, the CS solution for the dual problem in (10) is given as Algorithm 1.

Algorithm 1 Centralized subgradient algorithm

1: Establish some positive initial values for dual variable vectors $\boldsymbol{\mu}$ and $\boldsymbol{\nu}$ and fix a sufficient number of iterations i_{max} and step size $t^i = \frac{a}{b+i}$ where $a > 0, b > 0$.
2: Initialize the association of all users with a serving MBS / FBS. Each $k \in \mathbb{K}$ decides its serving BS $j \in \mathbb{J}$ on current dual variables $\boldsymbol{\mu}^i$ and $\boldsymbol{\nu}^i$ according to $j_k^i = \mathbf{argmax}_j \frac{B_j R_{k,j}}{\mu_j + \nu_k}$.
3: Calculate the number of users attached to the BS j for the i-th iteration and let it be K_j^i.
4: Update the dual variables μ_j^{i+1} and ν_k^{i+1} according to the current values of dual variables for the i-th iteration (μ_j^i and ν_k^i) by taking the partial derivative of (10) with respect to μ_j^i and ν_k^i respectively according to:
$\mu_j^{i+1} = \mathbf{max}((\mu_j^i + t^i(\sum_{k \in \mathbb{K}_j^i}(\mu_j^i + \nu_k^i)^{-1} - S_j)), 0)$ and $\nu_k^{i+1} = \mathbf{max}((\nu_k^i + t^i((\mu_j^i + \nu_k^i)^{-1} - 1)), 0)$.
5: Go to step 2 and continue while $i < i_{max}$.

Algorithm 1 presents a globally optimal solution for the convex dual problem (10) where during each iteration, the dual variables (Step 4) provide association based on the maximum throughput for each user (Step 2). However, the results observed may not be optimally feasible but nearby feasible for the primal problem (6) because of the distinct characteristic of the primal problem and limited number of iterations. The dual variables obtained by subgradient algorithm are nevertheless known to provide a near optimal solution for the primal problem [6].

---

[1]In the interest of space, the detailed derivation is not provided and can be obtained from the work in [12].

B. A Game Theoretical Distributed Approach for User-Cell Association

While CS approach maximizes sum-throughput to solve the optimization problem in (6), another approach which provides near optimal performance relies on load aware distributed decision making for user-cell association [12][23]. In this work, we formulate this distributed user-cell (DUC) association decision process in a new context, i.e mmWave massive MIMO. The modified DUC algorithm performs the association based on the max-throughput, i.e. each user aims to associate with a BS which maximizes its throughput in a selfish manner. In contrast to CS, this distributed non-cooperative game theoretical approach provides a low complexity implementation yet near optimal solution to (6) [12].

Consider a pertinent scenario where each BS is assumed to be associated with at least S_j users (indicating fully loaded BSs) in the network. In the DUC approach, a user tends to change its unique association configuration until there is no BS which yields better throughput. At this saturation point, all the users in the network reach an equilibrium point referred as "Nash equilibrium" (NE). When the scheduler operates in PF mode, every user uniquely reaches the NE if the distributed algorithm is performed selfishly [23]. The condition for the discussed NE using PF can be given by

$$\frac{B_j S_j R_{k,j}}{|K_j|} \geq \frac{B_l S_l R_{k,l}}{|K_l| + 1}, \quad \forall k \in \mathbb{K}, \forall j, l \in \mathbb{J}, l \neq j. \quad (11)$$

The DUC user-association algorithm is derived from [23] and presented as Algorithm 2.

Algorithm 2 User-centric Distributed algorithm

1: Initialize the iteration count and the number of migrations observed by all users as $i = 0$ and $\boldsymbol{m} = 0$ respectively. Fix a sufficient number of iterations i_{max} and a realistic switching probability p.
2: Every user $k \in \mathbb{K}$ updates its BS-association during each iteration and switches from its current serving BS k to a different BS l when the following conditions are met:
$\frac{B_l S_l R_{k,l}}{|K_l| + 1} > \frac{B_j S_j R_{k,j}}{|K_j|}$ and $rand < p^{(m_{i_k} + 1)}$.
3: During each iteration i, increment the migration count m_{i_k} for each k whenever k migrates from its current BS j to a different BS l (i.e. when conditions from Step 2 are satisfied).
4: Go to step 2 and continue while $i < i_{max}$.

It is seen from Algorithm 2 that the increment in the migration count m_{i_k} prevents frequent concurrent BS migrations of a user with an exponential decrease in migration probability (Step 2).

IV. EXPERIMENTAL EVALUATION

In this section, we evaluate the performance of the four user-cell association algorithms for massive MIMO deployment in a two-tier network under two different set ups: 1) HF-HF (both tiers operating in HF band) ; 2) HF-mmWave (MBSs operating in HF while FBSs in mmWave bands). As we will see in our results, due to the distinct channel properties of HF and mmWave spectrum, for same user-cell association schemes, we obtain contrasting gains under different deployment scenarios under consideration.

A. Network Model

We consider a downlink UDHN consisting of two MBSs having 100 antennas each with 46 dBm transmit power and randomly deployed 34 FBSs having 40 antennas each with 35 dBm transmit power in a rectangular region of dimensions 900m x 1800m. The MBSs are placed in the center of two square areas identifying hot-zones (higher user concentration) for the non-uniform user distribution in the simulation area. Each hot-zone contains about 1/3rd of the total user-count with the spatial distribution varying in each simulation run to provide more accurate results. The FBS deployment is uniform throughout the simulation area as shown in the network snapshot in Fig. 1. The MBSs, FBSs and users are represented by □, o and + respectively.
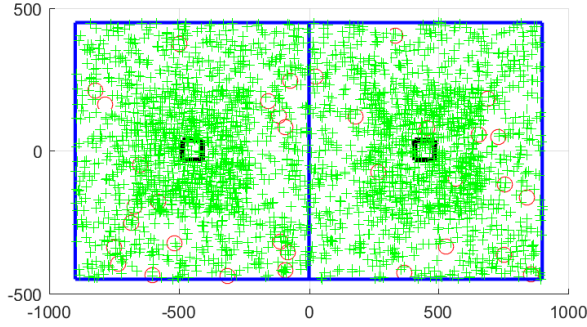

Fig. 1.   Network Layout.

We assume an intra-cell interference free network by allocating a set of 10 orthogonal pilots to be shared amongst the MBSs whereas the FBSs share a different set of 4 orthogonal pilots for channel estimation. A detailed list of simulation parameters is presented in Table II.

B. Throughput performance of user-cell association algorithms in mmWave massive MIMO

The throughput performance of the user-cell association algorithms under consideration for the mmWave massive MIMO UDHN is given in fig. 2. The 5 percentile throughput result in fig. 2a shows that the modified CS and DUC algorithms outperform the baseline association schemes. MR demonstrates the worst performance in terms of user throughput while figs. 2a, 2b and 2c reveal the indistinguishable performance of the CS and DUC algorithms. In fig. 2d, we compare the performance of the DUC and SPL by taking the ratio of their respective throughput statistics and plotting the CDF of the results obtained in each iteration. Gains are observed for each of the data rate statistics presented in figs. 2a, 2b and 2c. For instance, it is seen that for about 60% of the iterations, a gain of 20% is achieved in the 5 percentile data throughput.

To demonstrate why incorporating the bandwidth during user-cell association is indispensable for the HF-mmWave system considered, consider fig. 3 which depicts the 5 percentile throughput when spectral efficiency is optimized in the utility function maximization as done in [12]. It is clear from figs. 2a and 3 that with the effect of bandwidth taken out

TABLE II
SIMULATION PARAMETERS

Parameter	Value
Bandwidth, Carrier frequency of mmWave FBS	800 MHz 38 GHz
Bandwidth, Carrier frequency of HF MBS	20 MHz 2 GHz
Simulation area dimensions	900 m x 1800 m
Mean number of users	3000
Q , T	3, 7
N_F, T_K, k_b	7 dB, 290° Kelvin, 1.38×10^{-23} J/ Kelvin
Two-slope LOS path loss model of HF MBS	$22log(d) + 34.02 + X_\sigma$, $d < 320$m $40log(d) - 11.02 + X_\sigma$, $320 < d < 5000$m $\sigma = 4$ dB
NLOS pathloss model of HF MBS	$39.1log(d) + 19.56 + X_\sigma$ $\sigma = 6$ dB
Two-slope LOS path loss model of HF FBS	$22log(d) + 34.02 + X_\sigma$, $d < 120$m $40log(d) - 3.36 + X_\sigma$, $120 < d < 5000$m $\sigma = 3$ dB
NLOS pathloss model of HF FBS	$36.7log(d) + 30.53 + X_\sigma$ $\sigma = 4$ dB
Pathloss model of mmWave FBS	$20log(4\pi/\lambda) + 10\alpha_{LOS(orNLOS)} + X_\sigma$ LOS: $\sigma = 4.6$ dB, $\alpha_{LOS} = 1.9$ NLOS: $\sigma = 12.3$ dB, $\alpha_{NLOS} = 3.3$
$P_{LOS}(d)$ for mmWave FBS	$min(18/d, 1)(1 - e^{(-\frac{d}{36})} + e^{(-\frac{d}{36})})$
$P_{LOS}(d)$ for HF MBS	$min(18/d, 1)(1 - e^{(-\frac{d}{63})} + e^{(-\frac{d}{63})})$
Transmit power of MBS and FBS respectively	46 dBm 35 dBm
A_j for MBS, FBS	100, 40
S_j for MBS, FBS	10, 4
user height	1.5 m
BS height	FBS: 10 m, MBS: 25m
p	0.1
FBS radius	40 m

of the maximization function, CS and DUC perform worse than the SPL. This is due to significant SINR reduction specially for NLOS users that is compensated with higher available spectrum at mmWave. Hence, the modification in the optimization function in (6) is justified for our HF-mmWave massive MIMO UDHN system model.
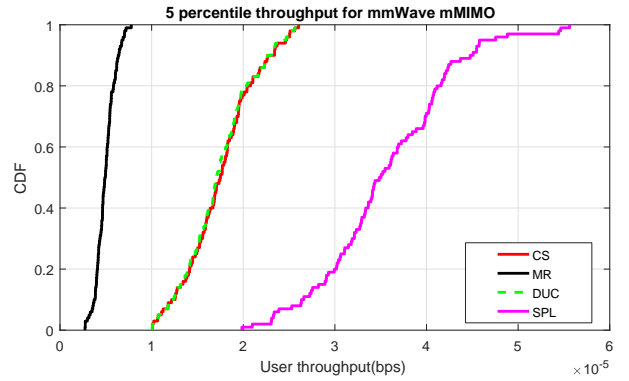

Fig. 3.   Throughput with spectral efficiency based user-cell association

C. Throughput gain with mmWave deployment at FBS tier

An interesting insight from our simulation results would be to analyze if operating FBS tier at the mmWave where there is a relative abundance of spectrum provides any notable throughput gains. While the throughput gradient (not presented in results due to limited space) showed that SPL had the
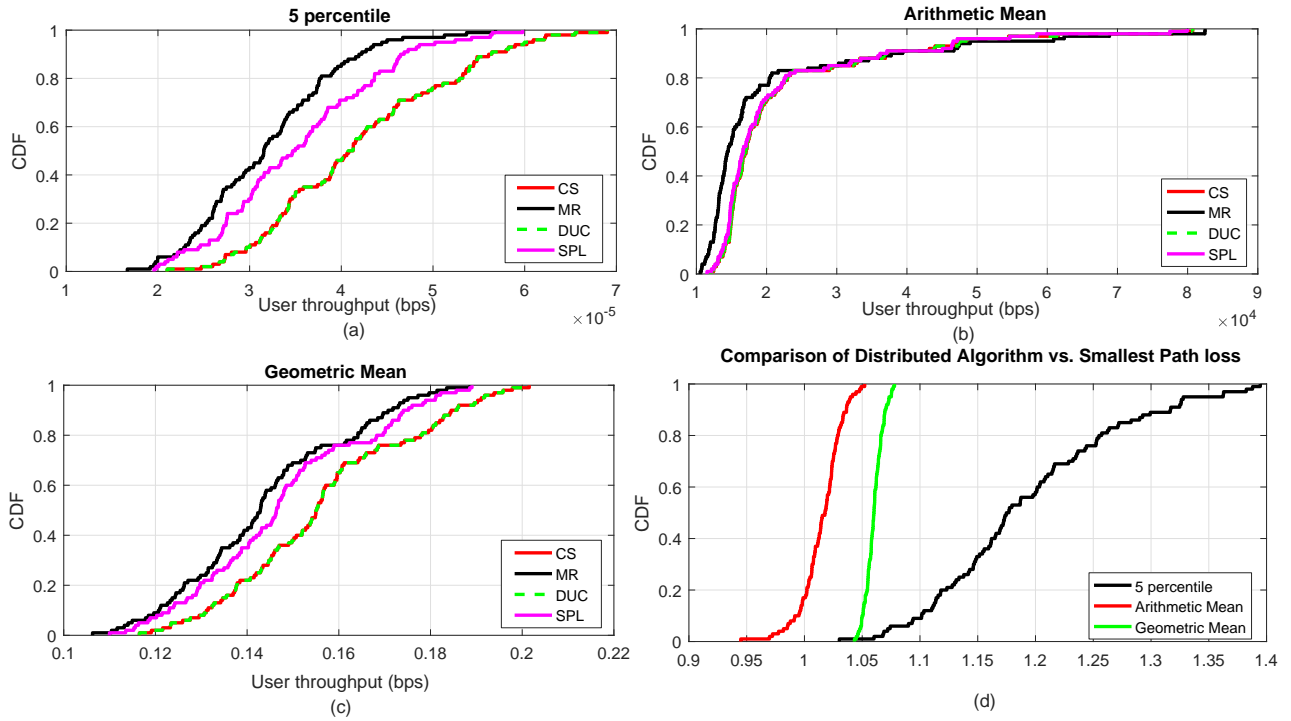
Fig. 2. Performance comparison of user-cell association algorithms for mmWave massive MIMO using PF

largest throughput percentage increase (approx. 50%) when the operating frequency is shifted from HF to mmWave, it is clear from fig. 4 that even the optimal CS and DUC yield 30% increase for almost half of the realizations. This consolidates the practical viability of HF-mmWave co-existence in UDHN massive MIMO systems.
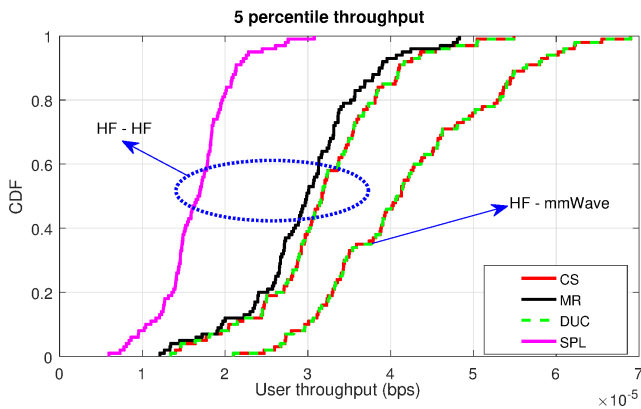

Fig. 4. Comparison of HF-HF versus HF-mmWave network

D. Load Distribution of the user-cell association schemes

Fig.5 presents the load association of users with the MBSs and FBSs under three user-cell association schemes. Note that since CS and DUC give near identical throughput and user-cell association patterns, we can only use one of these for analysis. Fig. 5 plots the number of users associated with each BS in descending order while clearly demarcating the

MBS and FBS tier association. In terms of offloading the MBSs, the DUC scheme clearly outperforms MR and SPL. MR association scheme exhibits the worst performance with highest net loads on the MBS tier. The results in fig. 5b reveal that DUC offers higher and more balanced user association with the FBS tier which eventually results in higher system throughput (see fig.2). While MR and SPL are blind towards cell loads during user-cell association, the load aware CS and DUC provide dual benefits of higher user throughput as well as decongestion of MBS tier by using the per user throughput as the association criteria.

V. CONCLUSION

In this paper, we present a comparative analysis of four different user-cell association algorithms for an ultra-dense multi-tier HetNet with massive MIMO deployment in both HF and mmWave spectrum. The four user-cell association algorithms analyzed in this paper include two optimal schemes namely: 1) centralized sub-gradient (CS) throughput max-imization based association and 2) distributed user-centric game theoretic (DUC) based association. Though the basic idea of both CS and DUC is inspired from earlier work [12] [23], we have adapted the optimization problem with a modi-fied utility function to incorporate idiosyncrasies of a mmWave based network. The benchmark approaches used for analysis include: 1) smallest pathloss (SPL) model and 2) max rate (MR). We investigated different key performance indicators including 5 percentile throughput, average throughput and inter-tier load distribution. Results indicate that both CS and DUC association algorithms outperform the baseline schemes
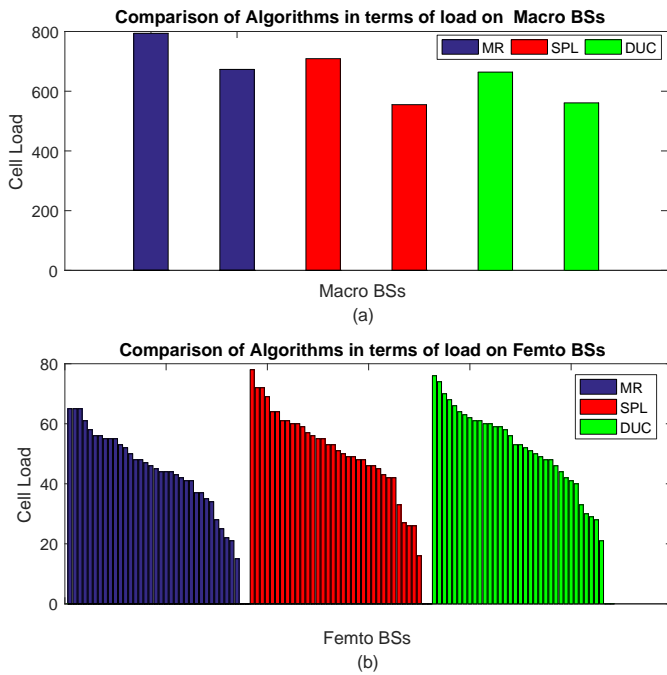
Fig. 5. Load Distribution for the user-cell association algorithms at HF-mmWave.

by virtue of higher throughput and efficient MBS off-loading. While the DUC association almost matches the performance of the CS approach, the simplicity in its implementation without requiring centralized optimization renders it as a suitable candidate for user-cell association in future mmWave massive MIMO networks.

REFERENCES

[1] Z. Pi and F. Khan, "An introduction to millimeter-wave mobile broadband systems," *IEEE Communications Magazine*, vol. 49, no. 6, pp. 101–107, June 2011.

[2] T. S. Rappaport, G. R. MacCartney, M. K. Samimi, and S. Sun, "Wideband Millimeter-Wave Propagation Measurements and Channel Models for Future Wireless Communication System Design," *IEEE Transactions on Communications*, vol. 63, no. 9, pp. 3029–3056, Sept 2015.

[3] F. Rusek, D. Persson, B. K. Lau, E. G. Larsson, T. L. Marzetta, O. Edfors, and F. Tufvesson, "Scaling Up MIMO: Opportunities and Challenges with Very Large Arrays," *IEEE Signal Processing Magazine*, vol. 30, no. 1, pp. 40–60, Jan 2013.

[4] H. S. Dhillon, R. K. Ganti, and J. G. Andrews, "Load-Aware Modeling and Analysis of Heterogeneous Cellular Networks," *IEEE Transactions on Wireless Communications*, vol. 12, no. 4, pp. 1666–1677, April 2013.

[5] S. Corroy, L. Falconetti, and R. Mathar, "Dynamic cell association for downlink sum rate maximization in multi-cell heterogeneous networks," in *2012 IEEE International Conference on Communications (ICC)*, June 2012, pp. 2457–2461.

[6] K. Shen and W. Yu, "Distributed Pricing-Based User Association for Downlink Heterogeneous Cellular Networks," *IEEE Journal on Selected Areas in Communications*, vol. 32, no. 6, pp. 1100–1113, June 2014.

[7] H. Pervaiz, L. Musavian, and Q. Ni, "Joint user association and energy-efficient resource allocation with minimum-rate constraints in two-tier HetNets," in *2013 IEEE 24th Annual International Symposium on Personal, Indoor, and Mobile Radio Communications (PIMRC)*, Sept 2013, pp. 1634–1639.

[8] D. Liu, L. Wang, Y. Chen, M. Elkashlan, K. K. Wong, R. Schober, and L. Hanzo, "User Association in 5G Networks: A Survey and an Outlook," *IEEE Communications Surveys Tutorials*, vol. 18, no. 2, pp. 1018–1044, Secondquarter 2016.

[9] J. G. Andrews, S. Singh, Q. Ye, X. Lin, and H. S. Dhillon, "An overview of load balancing in hetnets: old myths and open problems," *IEEE Wireless Communications*, vol. 21, no. 2, pp. 18–25, April 2014.

[10] H. T. Friis, "A Note on a Simple Transmission Formula," *Proceedings of the IRE*, vol. 34, no. 5, pp. 254–256, May 1946.

[11] T. Rappaport, R. Heath, R. Daniels, and J. Murdock, *Millimeter Wave Wireless Communications*, ser. Communication engineering and emerging technologies. Prentice Hall, 2014. [Online]. Available: https://books.google.com/books?id=_Tt_BAAAQBAJ

[12] D. Bethanabhotla, O. Y. Bursalioglu, H. C. Papadopoulos, and G. Caire, "Optimal User-Cell Association for Massive MIMO Wireless Networks," *IEEE Transactions on Wireless Communications*, vol. 15, no. 3, pp. 1835–1850, March 2016.

[13] D. Bethanabhotla, O. Y. Bursalioglu, H. C. Papadopoulos and G. Caire, "User association and load balancing for cellular massive MIMO," in *2014 Information Theory and Applications Workshop (ITA)*, Feb 2014, pp. 1–10.

[14] "Technical Specification Group Radio Access Network; Study on 3D Channel Model for LTE (Release 12), document 3GPP TR 36.873," *3GPP*, Sep. 2014.

[15] T. Bai and R. W. Heath, "Coverage and Rate Analysis for Millimeter-Wave Cellular Networks," *IEEE Transactions on Wireless Communications*, vol. 14, no. 2, pp. 1100–1114, Feb 2015.

[16] A. Molisch, *Wireless Communications*, ser. Wiley - IEEE. Wiley, 2010. [Online]. Available: https://books.google.com/books?id=vASyH5-jfMYC

[17] B. M. Hochwald, T. L. Marzetta, and V. Tarokh, "Multiple-antenna channel hardening and its implications for rate feedback and scheduling," *IEEE Transactions on Information Theory*, vol. 50, no. 9, pp. 1893–1909, Sept 2004.

[18] T. L. Marzetta, "Noncooperative Cellular Wireless with Unlimited Numbers of Base Station Antennas," *IEEE Transactions on Wireless Communications*, vol. 9, no. 11, pp. 3590–3600, November 2010.

[19] H. Q. Ngo, E. G. Larsson, and T. L. Marzetta, "Energy and Spectral Efficiency of Very Large Multiuser MIMO Systems," *IEEE Transactions on Communications*, vol. 61, no. 4, pp. 1436–1449, April 2013.

[20] S. Gimenez, S. Roger, P. Baracca, D. Martín-Sacristán, J. F. Monserrat, V. Braun, and H. Halbauer, "Performance Evaluation of Analog Beamforming with Hardware Impairments for mmW Massive MIMO Communication in an Urban Scenario," *Sensors*, vol. 16, no. 10, p. 1555, 2016. [Online]. Available: http://dx.doi.org/10.3390/s16101555

[21] B. Xu, Y. Chen, M. Elkashlan, T. Zhang, and K. K. Wong, "User association in massive MIMO and mmWave enabled HetNets powered by renewable energy," in *2016 IEEE Wireless Communications and Networking Conference*, April 2016, pp. 1–6.

[22] J. G. Andrews, T. Bai, M. N. Kulkarni, A. Alkhateeb, A. K. Gupta, and R. W. Heath, "Modeling and Analyzing Millimeter Wave Cellular Systems," *IEEE Transactions on Communications*, vol. 65, no. 1, pp. 403–430, Jan 2017.

[23] E. Aryafar, A. Keshavarz-Haddad, M. Wang, and M. Chiang, "RAT selection games in HetNets," in *2013 Proceedings IEEE INFOCOM*, April 2013, pp. 998–1006.